AN09: DQE Measurements for RadEye EV Sensors

Introduction

The EV series of RadEye sensors offers some unique capabilities for x-ray imaging systems, not only in terms of its extended energy response but also by combining high spatial resolution with an inherently low-noise detection process. These properties come to light in a series of DQE (detective quantum efficiency) measurements that study the signal-to-noise and resolution behaviour of this sensor. The DQE performance standard is used primarily in the medical industry, but the information presented can be readily applied to predict imaging performance in a variety of other applications as well.

The RadEye1 sensor manufactured by Rad-icon Imaging Corp. is a 512 by 1024 pixel CMOS photodiode array with a large active area of 24.6 by 49.2 mm and a pixel pitch of 48 µm. It is designed specifically for use with a direct-coupled scintillator in digital x-ray imaging (radiography) applications. The RadEye1 device is three-side buttable, so that larger imaging modules can be assembled by tiling several detectors in one or two dimensions. It can be used with a variety of different scintillators that can be directly deposited, bonded or simply pressed onto the detector surface. The scintillators that are most typically used with the RadEye1 sensor are Gd_2O_2S (Gadox) screens like Lanex® Fine or Min-R® Medium.

The EV series of the RadEye product line is unique in that it includes a fiber-optic faceplate (FOFP) that is bonded to the detector surface and integrated into the package. Typical faceplates are 3 mm thick and consist of 6-10 µm diameter fibers. The fiber size is small enough compared to the pixel size so that spatial alignment between fibers and pixels is not necessary. The function of the FOFP is to couple the output image from the phosphor screen to the photodiodes in the sensor with maximum coupling efficiency (>50% transmission) and minimal loss of spatial resolution. In addition, the FOFP also acts as an absorber of x-ray photons that penetrate past the scintillator and otherwise might be absorbed in the CMOS detector itself. X-ray photons that are absorbed directly by a photodiode contribute much more signal than those that are absorbed in the scintillator. This process manifests itself as additional noise in the image and leads to significant loss of signal-to-noise ratio at higher spatial frequency, and therefore to a reduction in DQE.

We have already presented DQE results for the standard RadEye sensor (without FOFP) in a previous application note (AN05: High-resolution CMOS imaging detector[1]). The following paper presents in detail the theory and measurement techniques used to determine detector DQE, and presents results specifically for the RadEye EV sensor for various x-ray energies and scintillator screens. We hope to present enough information so that these measurements can be duplicated for the same or for additional detector/screen combinations and measurement conditions.

DQE Theory

Detective quantum efficiency is defined as the square of the ratio of output signal-to-noise to input signal-to-noise:

$$DQE \equiv SNR_{out}^2 / SNR_{in}^2.$$

Given that the input signal consists of x-ray photons, which generally obey Poisson statistics, the input signal-to-noise ratio only depends on the number of x-ray quanta incident on the detector:

$$SNR_{in}^2 = q.$$

The output signal-to-noise ratio is commonly measured by observing the signal and the noise power spectrum at the detector output. The signal can also be expressed in terms of the input signal and the detector gain:

$$SNR_{out}^2 = S_{out}^2 / NPS = (q \cdot G)^2 / NPS.$$

Combining the above equations we get

$$DQE = q \cdot G^2 / NPS.$$

The detector gain and the noise power spectrum typically vary with spatial frequency. The modulation transfer function (MTF) is used to describe the relative decrease in gain with increasing spatial frequency. The final expression for calculating DQE then becomes

$$DQE(f) = q \cdot G^2 \cdot MTF(f)^2 / NPS(f).$$

Three of the four parameters in the above equations are readily measured simply by collecting enough images from the detector. The fourth, the input signal, is more difficult and usually requires the use of conversion tables and references. The accurate determination of q, and therefore G, is further complicated by the fact that the incident x-ray photons have different energies, and thus the conversion gain is at best an estimate of the average gain of the detector for a specific input spectrum.

Measurement Technique

The basic measurements required to determine the detector DQE are quite simple – only a handful of images are necessary to obtain a quick initial result. However, it is nevertheless very important to take special care in order to avoid experimental errors from influencing the results. This section describes the three performance criteria that need to be measured to calculate DQE: the Modulation Transfer Function, the Noise Power Spectrum, and the detector gain. In each case it also discusses potential pitfalls that can affect the outcome of the measurement.

MTF

Several techniques can be used to measure MTF. This author prefers the edge method, both for its mathematical simplicity and for ease of measurement. However, the computational algorithm is a bit complicated if oversampling and averaging are utilized.

In the edge MTF technique, a "knife edge" made of a thin piece of strongly absorbing material is placed directly onto the detector and aligned at a slight angle (typically 5-10°) to either the row or column direction. The edge should be as straight as possible (to within a fraction of the pixel size) and also as thin as possible to minimize shadowing in an off-axis measurement and scatter from the edge material at higher energies. A 0.5 mm thick piece of tungsten was used in our experiments. For an accurate measurement a contrast of 1000:1 or higher between the unobscured and the blocked parts of the image is desirable. Using a lower contrast may obscure some of the details of the edge response and yield an inaccurate result.

The measurement itself simply consists of taking an offset- and gain-corrected image of the edge using an appropriate combination of source kV, mA and integration time. It may be useful to average several frames in order to reduce the shot noise in the image. The measurement should be repeated using several different placements of the edge in order to determine variations across the detector or between the horizontal and vertical directions.

Once an image has been obtained, the first step of the analysis is to differentiate it along the row- or column-direction that is perpendicular to the edge. A plot of signal values along that direction reveals the line spread function (LSF) of that particular row or column. The exact position of the edge in the image can now be determined by calculating a least-square fit through the locations of the LSF maxima. This is important because for the next step – the oversampling – the edge position needs to be known with sub-pixel accuracy.

Oversampling is necessary in order to determine the true shape of the LSF, which may only be a few pixels wide at its half-maximum level. Let's assume the edge is aligned along the column direction. Then for each row, the edge crosses the detector pixel in a slightly different location. Consequently, the LSF measured on that row is sampling the "true" continuous LSF with a slight phase shift with respect to neighboring rows. By taking into account the varying phase shifts over many rows a continuous LSF can be pieced together. In practice it is easier to subdivide each pixel into a number of sub-pixels and simply determine which sub-pixel the edge crosses in each row. The data from each row can then be aligned with one particular sub-pixel, and by averaging sub-pixels over many rows an oversampled LSF is obtained. It is important to keep the angle between the edge and the column at a minimum because we are assuming that the edge crosses the pixel at one particular location. A larger angle would cause blurring of the LSF and a subsequent reduction in MTF.

The final step of the measurement is to take the Fourier Transform of the LSF in order to obtain the MTF for the detector. Because of the oversampling we end up with MTF information beyond the Nyquist limit of the detector, which can be discarded. The resulting MTF is often called the "presampled MTF" of the detector because the effects of the sampling detector response (such as aliasing) have been removed. The actual contrast, of course, depends strongly on the phase shift between the object and the detector, and may be significantly less.

NPS

The Noise Power Spectrum can be obtained by applying a two-dimensional Fourier Transform to an offset- and gain-corrected image from the detector. However, it is very important to remove fixed pattern variations from the image because they can easily influence the obtained spectrum. A simple method to accomplish this is to obtain two consecutive images from the detector and subtract them. When doing this the noise variances of the two images add, so the resulting NPS has to be scaled by a factor of two.

NPS data are inherently noisy and require averaging over several hundred data sets in order to obtain a reasonably smooth curve. If the two-dimensional NPS is symmetric, the analysis may be limited to either the row or the column direction by applying a one-dimensional Fourier Transform and averaging in the other dimension. This method yields a usable NPS curve from a single pair of images. It should be noted that the zero-frequency or DC value of the NPS is proportional to the average signal level in the difference image. Since there is always some small amount of DC fluctuation between the images, this value should be discarded.

X-Ray Flux and Detector Gain

By far the most difficult component in calculating the detector DQE is determining the x-ray quantum flux that is incident on the detector. Unless one has access to an x-ray spectrometer that can be used to characterize the energy spectrum of the x-ray source, it is usually necessary to rely on physical models of the x-ray spectrum from a typical x-ray tube. Several sources of x-ray spectra can be found both in the literature and on-line. For this study we made use of the Siemens X-Ray Toolbox[2], which is based on models developed by John Boone at UC Davis[3-5].

The output spectrum of the x-ray source needs to be adjusted for any absorbing materials in the x-ray path such as the volume of air between the source and the detector, and any beam-hardening filtration layers. The magnitude of the resulting quantum flux then needs to be calibrated against an actual measurement taken at the position of the detector in the experiment. A typical way of accomplishing this is to measure the exposure (in roentgens) using a simple ion chamber detector. This can then be converted to grays or air kerma as required, keeping in mind that the measurement is made in air.

Once the incident quantum flux has been obtained, the x-ray spectrum can be integrated and scaled to the pixel area in order to determine the number of x-ray photons incident per pixel. The detector gain is then simply the average signal level from the image that was used to calculate the NPS divided by the number of photons. It should be noted that this gain actually varies both on a pixel-by-pixel basis as well as with the energy of the incident photon. For practical purposes, however, an average gain value can be used. This gain value combines the detection efficiency of the scintillator (number of photons absorbed), the conversion efficiency of the scintillator/detector combination (electrons collected per photon), and the conversion gain of the detector (ADU/electron). The output signal (and the conversion gain) carries the same units as the NPS since it is measured from the same images.

Experimental Results

All measurements were made using a Shad-o-Snap 1024 EV camera. This camera contains a RadEye2 EV sensor module with a 1000-row by 1024-column CMOS detector. The sensor module can be fitted with different scintillators. In this case we made measurements using the standard Min-R Medium scintillator as well as the optional Lanex Fine screen. The camera electronics can be modified to provide different gain settings. The standard version of the Shad-o-Snap camera has an electronic gain of 5x between the sensor output and the A/D converter. We also tested a "high-gain" version of the camera electronics which provides a gain of 22x. The read noise of the high-gain camera is approximately 150 electrons rms (referred back to the detector pixel), whereas the standard camera read noise is 250 electrons rms (dominated by the quantization noise of the ADC).

All measurements were made using an Oxford XTC5010 source with a tungsten target and a 0.125 mm beryllium exit window. A 0.5 mm aluminum filter was placed below the source to harden the beam. Further beam hardening

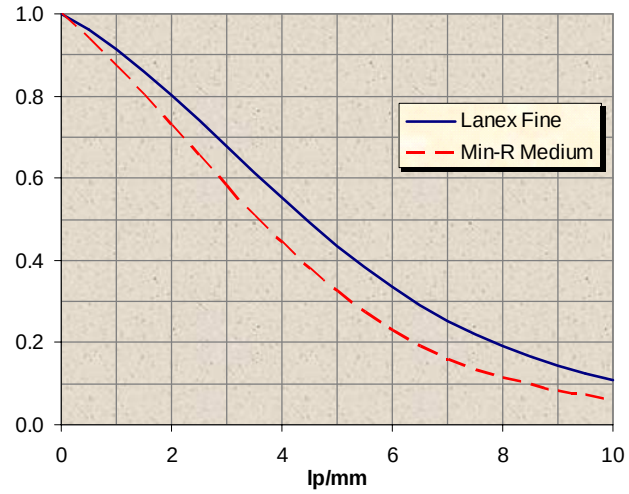

Figure 1 – RadEye EV MTF.

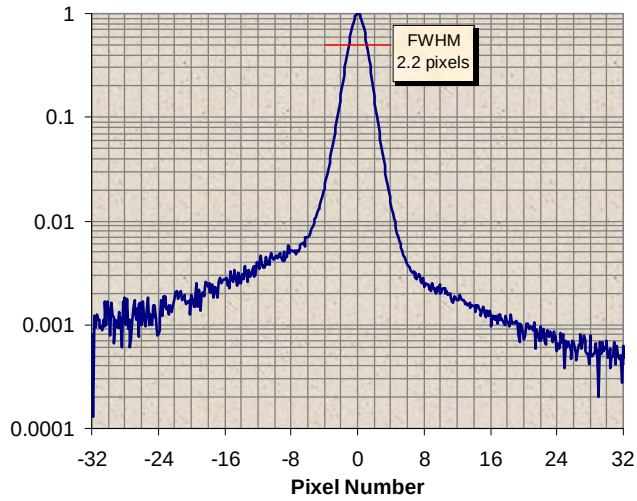

Figure 2 – Typical Line Spread Function (LSF).

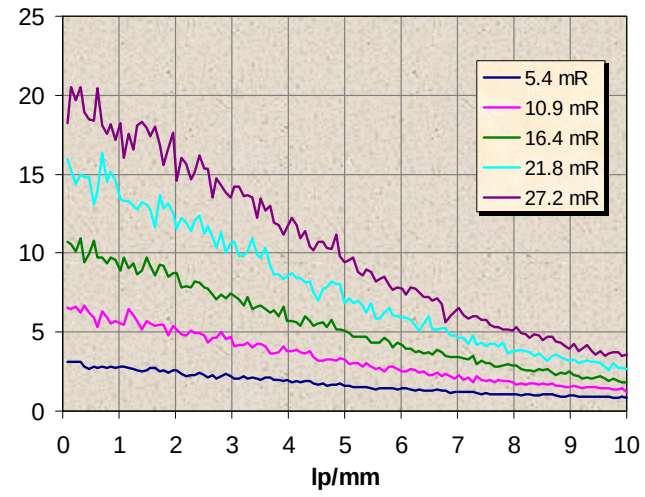

Figure 3 – Typical Noise Power Spectrum (NPS).

was obtained from the 350 mm air path between the source and the detector. The quantum flux calibrations were performed using a 180 cc ion chamber and a RadCal 2026C dosimeter.

The MTF of the RadEye EV sensor is shown in Figure 1 for both types of scintillator. Since the measured MTF can vary by a few percent across the detector surface, the curves shown represent an average of several measurements at various locations on the detector. There is no significant difference between the MTF along the row direction and that along the column direction. Figure 2 shows a typical line spread function for one of the edge images obtained using Min-R Medium. The signal from the "light" side of the edge (left side of the graph) is noisier due to the x-ray shot noise in the image.

Noise power spectra were measured for various exposure levels and kV settings, using the procedure outlined in the previous section. Figure 3 shows a typical set of NPS curves. The general shape of the NPS curves follows that of the detector MTF. Figure 4 shows a two-dimensional NPS obtained for a 512x512 pixel image segment, illustrating the basic symmetry of the noise spectrum. The noise is essentially uncorrelated along both the row and column directions.

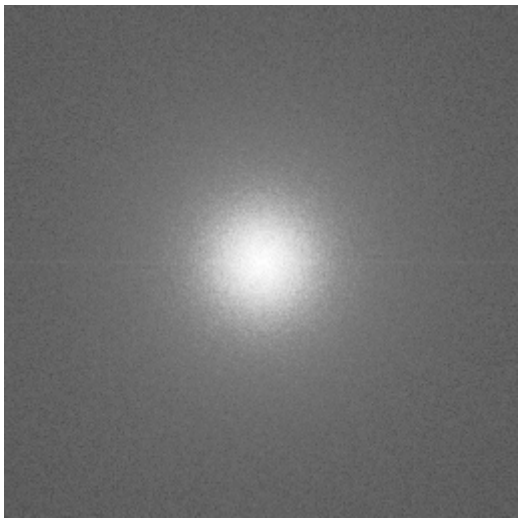

Figure 4 – 2D Noise Power Spectrum.

The resulting DQE curves are shown in the figures to the right. Figure 5 shows the energy dependence of the DQE over the 24 to 38 kVp range. These measurements were taken using the Min-R Medium screen at an exposure level sufficiently high to ensure that the sensor was quantum-noise limited (~40 mR). The detector has nearly perfect DQE at low energies where the scintillator absorbs almost every photon, and scales with the absorption efficiency of the screen as the x-ray energy increases.

Figure 6 compares the two scintillator screens for source settings of 24 kVp and 30 kVp. In each case several photon-noise limited curves were averaged together to improve the visibility of the data. The graph shows that even though Lanex Fine has a higher MTF than Min-R Medium, the lower absorption efficiency of the thinner scintillator results in an overall lower DQE, except for a small advantage in the 6-10 lp/mm range.

Finally, Table 1 summarizes the experimental parameters. Exposures between 5 and 50 mR were used to gather these data. We were unable to measure any significant change in DQE vs. exposure over this range, which is an indication that the camera noise is not influencing the measurement. In addition, there does not appear to be a significant performance benefit in using the high-gain camera electronics compared to the standard electronics, except perhaps at very low exposures where the camera read noise begins to have an effect.

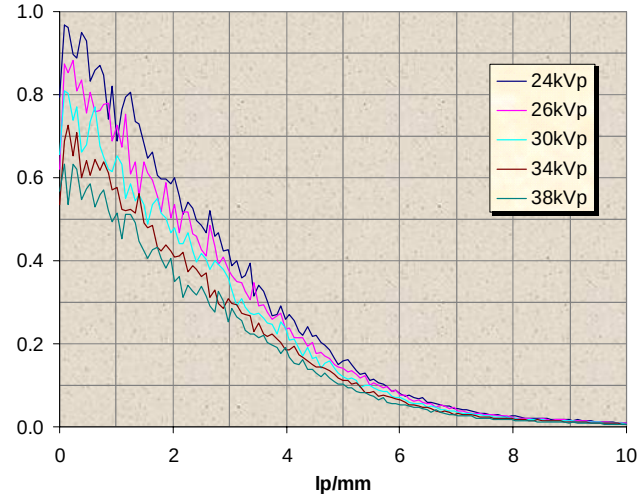

Figure 5 – DQE vs. X-Ray Energy.

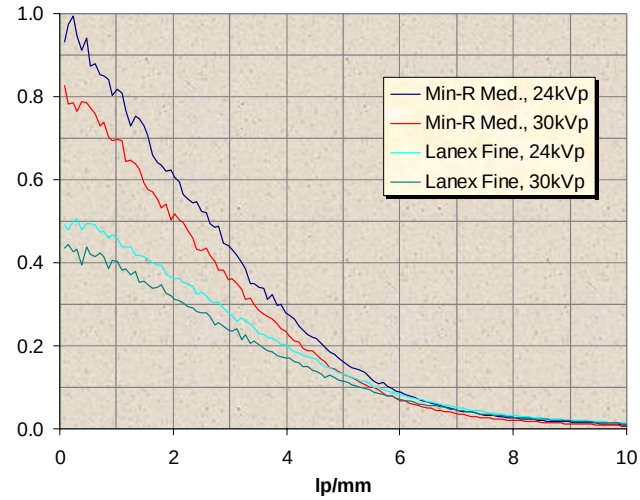

Figure 6 – DQE for Min-R Medium and Lanex Fine.

x-ray energy (kVp)	24	30	38	24	30	24
exposure (mR)	44.6	39.0	32.7	29.8	32.6	29.8
number of photons (N)	6537	7299	7902	4358	6121	4358
scintillator type	Min-R	Min-R	Min-R	Lanex	Lanex	Min-R
camera electronics	standard	standard	standard	hi gain	hi gain	hi gain
avg. signal (ADU)	264	303	307	328	519	715
rms noise (ADU)	1.90	2.27	2.49	4.45	6.36	6.05
gain (ADU/photon)	0.040	0.040	0.040	0.075	0.085	0.164

Table 1 – Experimental parameters.

Conclusion

The experimental results presented in the preceding sections indicate that the use of a thicker scintillator such as Min-R Medium is preferable over Lanex Fine. The key to understanding this is that, for the pixel size of this particular detector, the Min-R Medium screen is a better match than Lanex Fine. Lanex Fine is thin enough (~34 mg/cm^2) to provide good contrast to 20 lp/mm – well beyond the Nyquist limit of the RadEye1 detector. Min-R Medium, on the other hand, was designed for use up to 10 lp/mm. It has almost twice the x-ray cross-section (50-60 mg/cm^2), which means that it is able to achieve >90% DQE at low x-ray energies, and significantly higher DQE than Lanex Fine at higher energies where the absorption efficiency starts to decrease. Even though the MTF is lower, the improved absorption efficiency compensates for the reduced resolution over nearly the entire spatial frequency range.

A less obvious conclusion is that the addition of the FOFP results in a significant improvement in DQE. However, this statement is not so surprising given that the reduction in signal-to-noise due to direct absorption of x-rays in the photodiodes has been shown to seriously degrade DQE. The noise power decreases by nearly a factor of ten at the Nyquist limit as a result of adding the FOFP. This improvement comes despite the fact that the light output from the scintillator is attenuated by up to 50%, and the MTF reduced by as much as 5%. As an added benefit, the FOFP also improves the life expectancy of the sensor by reducing the harmful side-effects of direct x-ray absorption in the CMOS circuitry.

It should be noted that these results are somewhat specific to the type of x-ray tube being used. An x-ray generator with a molybdenum target produces a spectrum with slightly lower average energy, which would favor the Lanex Fine screen. However, we do not believe that the difference is significant enough to affect these results. The same precautions apply to using an unfiltered beam with a softer x-ray spectrum.

As a final note we point out that for most of these experiments the detector was quantum-noise limited. The main reason for this is that it only takes a few tens of x-ray photons to achieve this condition. However, at exposure levels below 5-10 mR we did notice a slight drop-off in DQE. Further experiments might be necessary to explore this behaviour and to fully characterize the low-signal limitations of the RadEye EV sensor.

References

1. T. Graeve, G.P. Weckler, “High-resolution CMOS imaging detector”, *Proc. SPIE* **4320**, 68-76, 2001.
2. http://www.healthcare.siemens.com/med/rv/toolbox/default.asp.
3. John M. Boone, Anthony Seibert, “An accurate method for computer-generating tungsten anode X-ray spectra from 30 to 140 kV”, *Medical Physics* **24**(11), 1661-1670, 1997.
4. John M. Boone, Thomas R. Fewell, Robert J. Jennings, “Molybdenum, rhodium, and tungsten anode spectral models using interpolating polynomials with application to mammography”, *Medical Physics* **24**(12), 1863-1874, 1997.
5. John M. Boone, “Spectral modeling and compilation of quantum fluence in radiography and mammography”, *Proc. SPIE* **3336**, 592-601, 1998.